Inorganic electrolyte additives to suppress the degradation of graphite anodes by dissolved Mn(II) for lithium-ion batteries

S. Komaba[a,*], B. Kaplan[a,b], T. Ohtsuka[a], Y. Kataoka[a], N. Kumagai[a], H. Groult[b]

[a]*Department of Chemical Engineering, Iwate University, Morioka, Iwate 020-8551, Japan*
[b]*Pierre and Marie Curie University, LI2C Laboratory, CNRS UMR 7612, 4 Place Jussieu, F 75252 Paris Cedex 05, France*

Abstract

It is well known that when the carbon/LiMn$_2$O$_4$-based cathode battery was operated at elevated temperatures, the severe capacity loss occurred in following cycles. As we recently described, the capacity loss is mainly due to the degradation on the carbon anode side caused by the deposition of manganese at the carbon followed by the irreversible decomposition at the graphite/deposited Mn/electrolyte interface. It was found that inorganic additives in electrolyte, such as LiI, LiBr, and NH$_4$I, effectively suppressed the degradation of graphite anode to improve the battery performance. In case of LiI and LiBr, the irreversible reaction at the Mn/electrolyte interface was suppressed by specific adsorption of iodide or bromide anions on the metallic Mn surface. Further, the reduction of Mn(II) would be suppressed by adding NH$_4$I into electrolyte which could be due to the formation of a stable amine complex of Mn(II).
© 2003 Elsevier Science B.V. All rights reserved.

Keywords: Lithium-ion battery; Graphite; LiMn$_2$O$_4$; Mn dissolution; Additive; SEI

1. Introduction

In the carbon/(spinel LiMn$_2$O$_4$) battery, manganese dissolution from the spinel occurs at high temperature (>50 °C), and some mechanisms of the Mn dissolution and its suppression methods were addressed by some groups [1–6]. We recently emphasized that the carbon anode was predominantly degraded by the dissolution of manganese in the carbon/LiMn$_2$O$_4$ system [7,8]. After the dissolution of manganese species from spinel LiMn$_2$O$_4$ at higher temperature, the soluble manganese species will reach the carbon anode, and then the ionic manganese, Mn(II), is readily reduced on the carbon because the standard redox potential of Mn/Mn(II) (ca. 1.8 V versus Li/Li$^+$) is much higher than that of the lithium intercalation into graphite. We concluded that the higher temperature degradation (>50 °C) in the carbon/LiMn$_2$O$_4$ system was mainly caused by the degradation on the anode side. Therefore, we believe that solving the problem of this anode deterioration is very important for enhancement of the entire carbon/LiMn$_2$O$_4$ system for hybrid and pure electric vehicles (HEV and PEV, respectively).

In order to improve the negative electrode performance in lithium-based secondary batteries, some organic/inorganic additives are known to be effective, such as CO$_2$ [9], HF [10,11], HI [12], AlI$_3$, and MgI$_2$ [13,14] for metallic lithium, and ethylene sulfite [15], vinylene carbonate [16–18], and chloroethylene carbonate [19] for carbon anode. In these cases, the effect on the solid electrolyte interface (SEI) formation plays a key role in determining the battery performance. On the side of spinel type LiMn$_2$O$_4$ cathode, though suppression of Mn(II) dissolution from the spinel is essentially important for enhanced performance, the "Mn dissolution-free" would be still difficult to solve the degradation problem of the C/(spinel Li–Mn–O) cell to our knowledge. In the C/(spinel Li–Mn–O) system, therefore, a protection of the negative electrode from soluble Mn(II) in an electrolyte is considered to be important and useful for understanding and improving the battery performance. In this study, we investigated the graphite anode performance in electrolytes containing small amount of LiI, LiBr, and NH$_4$I in order to suppress the Mn(II) reduction (Mn electrodeposition) and the drastic decomposition of electrolyte on deposited Mn surface.

2. Experimental details

Reagent grade natural graphite (Nakalai Tesque Inc., purity 99%, average particle size 10 μm), manganese(II) perchlorate, metallic manganese, LiI, NH$_4$I (Aldrich), and

LiBr (Kanto Chemical Co. Inc.) were used. Battery grade lithium metal foil, $LiClO_4$, ethylene carbonate (EC) and diethyl carbonate (DEC) were used as received.

For preparation of the working electrodes, natural graphite was used as the active material without any pretreatment, and *N*-methyl pyrrolidone (NMP) was added to the mixtures of the graphite (about 10 mg) and poly(vinylidene fluoride) as a binder in a weight ratio of 9:1. This mixture was ground and pasted onto a nickel net (13 mm in diameter), and dried at 100 °C for 1 day to remove the NMP ingredient. After drying, the electrode was pressed and then vacuum dried at 90 °C for one night. Lithium foils were used for both the reference and counter electrodes. Electrochemical tests were undertaken at 25 ± 2 °C in an Ar atmosphere. The charge–discharge tests were carried out between 0.02 and 1.5 V versus Li/Li^+ at a constant current density of 0.1 mA cm^{-2}. The reference and counter electrodes were isolated by a glass filter in another compartment filled with an additive-free electrolyte solution in order to avoid any side reaction of the additives with lithium metal and maintain a reliable reference potential for Li/Li^+ [8]. For comparison, a metallic manganese chip was used as the working electrode. The volume of the electrolyte solution in the working electrode compartment was ca. 14 cm^3. The electrolyte used was 1 mol dm^{-3} $LiClO_4$ EC + DEC (1:1 v:v). Before electrochemical cycling, small amounts of LiI ([I] = 500 ppm), LiBr ([Br] = 500 ppm), and NH_4I (8.3 mmol dm^{-3}; $[NH_4]$ = 150 ppm, [I] = 1050 ppm) used as an additive were dissolved into electrolyte solutions. Soluble Mn(II) perchlorate (150 ppm Mn(II)) was added after the fifth discharge (before the sixth charge) [8]. The hydrates used as additives were dried at 100 °C in a vacuum for 1 day more to remove any hydrated water prior to the addition. The surface of the electrode was observed using scanning electron microscopy (SEM) after drying electrode in air at 80 °C.

3. Results and discussions

It was confirmed that a graphite electrode showed typical charge–discharge performance in Mn(II)-free electrolyte solution; reversible capacity was ca. 340 mAh g^{-1} with high coulombic efficiency (nearly 100%) except for the first cycle that agrees with the reductive decomposition of the electrolyte including SEI formation. When Mn dissolution into electrolyte occurs in a practical graphite/(spinel Li–Mn–O) cell after several cycles, the graphite electrode is already modified with the SEI layer. As reported previously, we have investigated the influence of Mn(II) on the performance of the graphite modified with SEI. However, the SEI layer did not protect the graphite from the soluble Mn(II), and the decomposition of electrolyte was accelerated resulting in high irreversible capacity at sixth cycle (coulombic efficiency <20%) [8].

This degradation was successfully suppressed by pre-addition of LiI and LiBr into an electrolyte solution.
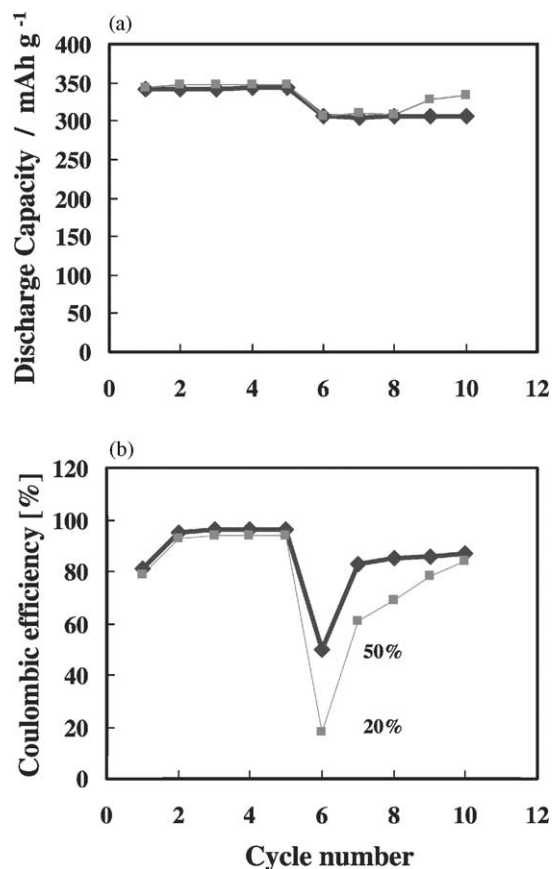

Fig. 1. Variation in (a) discharge capacity and (b) coulombic efficiency of a graphite electrode in 1 mol dm^{-3} $LiClO_4$ EC–DEC (1:1) containing LiI (as 500 ppm I) (thick line) and no additive (thin line). Manganese perchlorate (150 ppm Mn(II)) was added into the electrolyte before the sixth charge.

Figs. 1 and 2 show variations in discharge capacity and coulombic efficiency of a graphite electrode in $LiClO_4$/EC–DEC solution containing LiI and LiBr additive, respectively. In this test, Mn(II) was added after fifth discharge (before sixth charge), i.e. after SEI formation. In case of additive-free electrolyte, Mn(II) was electrochemically reduced on the graphite during the sixth charge followed by the drastic decomposition at electrolyte/deposited Mn/graphite interface, which brought about large irreversible capacity resulting in quite low efficiency of 20%. Note that when manganese dissolution occurs in the practical graphite/$LiMn_2O_4$ the whole discharge capacity of the battery will be severely degraded by the graphite anode limit, because of the capacity balance of positive/negative sides in the practical cell as we described previously [8]. However, the pre-addition of iodide or bromide is effective in suppression of the irreversible reaction. The efficiency at the sixth cycle was improved from 20 to 50% and 77% by adding a small amount of LiI or LiBr, respectively, into an electrolyte. Increasing the efficiency, the graphite exhibited a discharge capacity of 300 and 270 mAh g^{-1} in LiI and LiBr added electrolyte, respectively, even after the Mn(II) addition. The existence of halogen anions in an electrolyte influences the
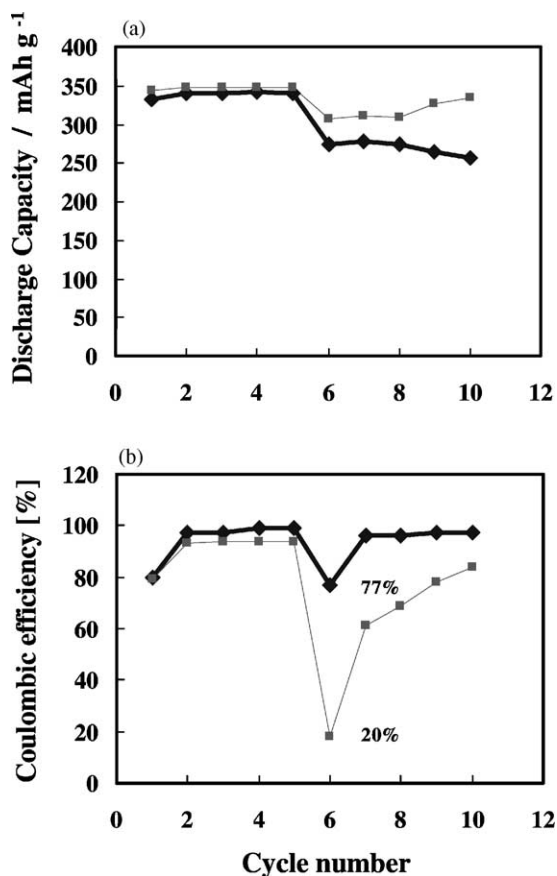
Fig. 2. Variation in (a) discharge capacity and (b) coulombic efficiency of a graphite electrode in 1 mol dm^{-3} LiClO$_4$ EC–DEC (1:1) containing LiBr (as 500 ppm Br) (thick line) and no additive (thin line). Manganese perchlorate (150 ppm Mn(II)) was added before the sixth charge.

Fig. 3. Cyclic voltammograms of a Mn electrode at 0.1 mA s^{-1} in 1 mol dm^{-3} LiClO$_4$ EC–DEC (1:1) with (solid line) and without (dashed line) LiI.

SEI formation process on the graphite surface, and it might form a highly ion-conductive layer [20]. Furthermore, addition of LiI is effective in improving cyclability of Li metal anode as reported by Ishikawa et al. [13]. In this case, physical adsorption of the iodide anion on the Li surface inhibited an interfacial reaction between Li and electrolyte. In order to clarify interaction between Mn metal and iodide anions, electrochemical behavior of metallic manganese electrode was examined in electrolyte solution with and without LiI.

Fig. 3 shows the cyclic voltammograms of Mn electrodes in LiI added and LiI-free electrolytes. In general, no alloy formation is known to occur with Li and 3d transition metals such as Mn. Obviously, the high (electro)chemical reactivity of electrolyte decomposition below 0.3 V was promoted on the metallic Mn surface in the LiI-free EC–DEC electrolyte as illustrated in Fig. 3. As mentioned above, Mn(II) was electrochemically reduced on the graphite during the sixth charge followed by the drastic decomposition at the electrolyte/deposited Mn/graphite interface, and consequently, the efficiency at the sixth became much lower due to the irreversible reactions. On the contrary, the LiI addition effectively suppressed the decomposition because reductive/oxidative current hardly flows in the voltammogram
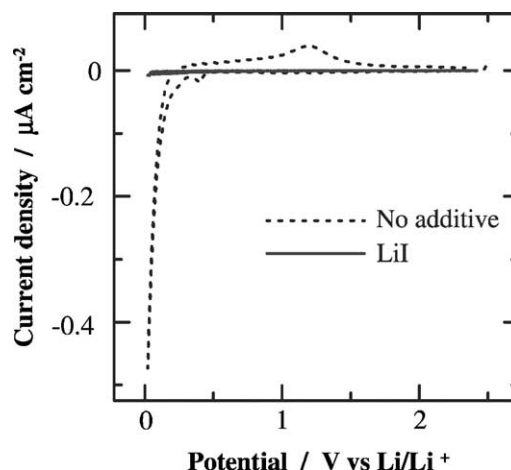
in the wide potential region between 0 and 2.5 V. It is likely that the specific adsorption of iodide on the Mn surface inhibited any electrochemical reactions including this interfacial decomposition. When manganese was deposited on the graphite surface during the charging as seen in Figs. 1 and 2, the iodide anion simultaneously adsorbed on the deposited Mn as seen from the voltammetry investigation. As a result, the electrolyte decomposition at the interface was suppressed by adsorption of iodide and bromide anions on the Mn surface deposited on the graphite, and the efficiency at the sixth cycle was improved from 20 to 50% by LiI addition. A similar mechanism could exist for the improvement by LiBr addition. When other compounds containing iodine were added into an electrolyte solution, the efficiency and reversible capacity were also improved. Although the manganese dissolution results in the remarkable capacity loss in a practical cell, these additives in an electrolyte would suppress the capacity loss although iodide ion will be decomposed (oxidized) at the LiMn$_2$O$_4$ positive electrode.

The graphite electrodes after the 10th discharge were examined by SEM as shown in Fig. 4. After dissolving 150 ppm of Mn(II) in an electrolyte containing no additive after five cycles, graphite particles are not observed at all since much thick deposit covers the electrode surface which was visible to the naked eye. The deposit comes mainly from the drastic decomposition at the interface after the manganese deposition. It is apparent that the degradation of graphite anode performance was due to this deposit preventing lithium intercalation. The amount of the deposits decreased as expected from the electrochemical results, and the morphology of the electrodes differs by additives. This fact agrees with the suppression effects by specific adsorption of iodide and bromide on the Mn surface as discussed for Fig. 3. Furthermore, the morphology was different between the LiI and LiBr. In case of LiBr, some small particles of <1 µm were deposited and dispersed on
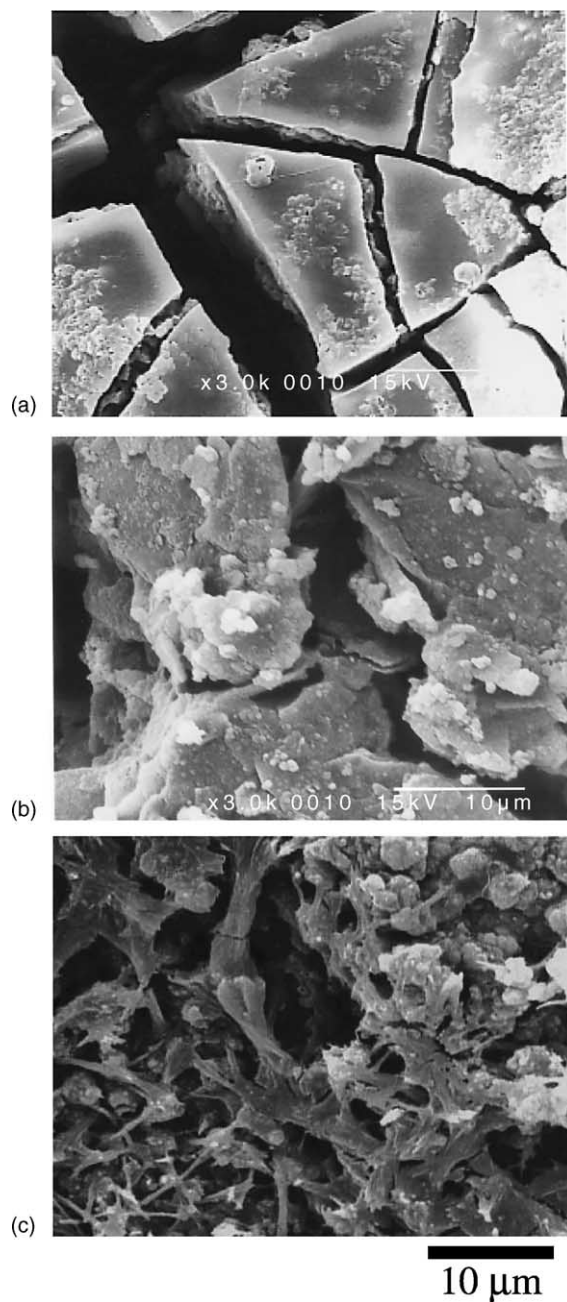
Fig. 4. SEM pictures of graphite electrode surface after 10 cycles in 1 mol dm^{-3} LiClO$_4$ EC–DEC containing (a) no additive, (b) LiBr and (c) LiI.

Fig. 5. (a) Charge–discharge curves and variation in (b) discharge capacity and (c) coulombic efficiency of graphite electrode in 1 mol dm^{-3} LiClO$_4$ EC–DEC (1:1) containing NH$_4$I ([NH$_4$] = 150 ppm, [I] = 1050 ppm) (thick line) and no additive (thin line). Manganese perchlorate (150 ppm Mn(II)) was added before the sixth charge.

the surface of graphite particles while mesh-like deposits appeared for LiI system. This difference of the morphology would be due to the original SEI, which might incorporate each additive and whose composition and structure were influenced by the additives [12] and chemically bonded iodine [21]. It is likely that the adsorption properties should be different between iodide and bromide. Accordingly, the SEI formation and the Mn(II) degradation was influenced by existence of LiI or LiBr in an electrolyte.

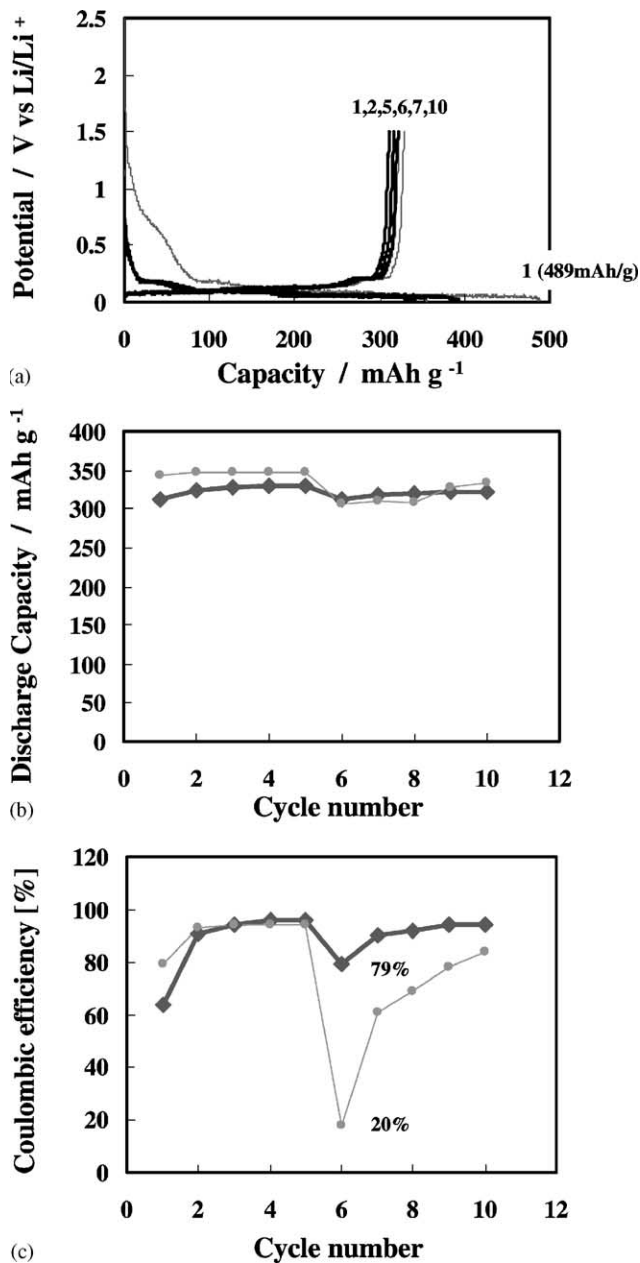In general, many transition metal ions form ammonia complex compounds, and their deposition potential from the complex ions in an aqueous medium becomes lower compared to that calculated from Nernst equation as transition metal ions are stabilized by coordinate bond with ammonia ligands. In order to suppress the degradation more effectively, furthermore, Fig. 5 shows variation in discharge capacity and efficiency in an NH$_4$I dissolved electrolyte where Mn(II) was also added after the fifth discharge. It is expected that NH$_4^+$ ions are effective in suppressing Mn deposition by forming Mn(II)–amine complex in combination with the iodide effect. Clearly, the degradation by Mn(II) addition after the fifth cycle was more effectively

suppressed by NH$_4$I compared to those for LiI and LiBr. The sixth cycle efficiency, which is the important factor in a practical cell as mentioned above, was remarkably improved from 20 to 79%. Furthermore, the charge–discharge curves and discharge capacity are hardly changed even after Mn(II) addition. During the initial five cycles, the discharge capacity was slightly decreased by NH$_4$I addition, and the initial efficiency was decreased comparing to that in NH$_4$I-free electrolyte. It is likely that reduction of ammonium ions and/or protons caused irreversibly. There remain problems for practical use that these additives will be oxidized at the cathode because the redox potential, E^0 of I$_2$/I$^-$ = ca. 3.6 V versus Li/Li$^+$, is lower than LiMn$_2$O$_4$ operation potential. This is, however, the first study on effective additives in suppressing the degradation of graphite anode on the basis of our previous investigation [8]. Further analyses of these additive system and investigation of effective methods for the suppression are in progress by modification of the carbon electrode.

4. Conclusion

In order to improve the carbon/LiMn$_2$O$_4$ battery performance, some inorganic additives into electrolyte were investigated for the suppression of irreversible reaction at the graphite anode, i.e. the capacity loss of the practical cell. In case of LiI and LiBr, the irreversible decomposition at the graphite Mn/electrolyte interface was suppressed by specific adsorption of iodide or bromide anion on the metallic Mn surface. In case of NH$_4$I, the reduction of Mn(II) was also suppressed by formation of a stable amine complex of Mn(II).

Acknowledgements

References

[1] D.H. Jang, S.M. Oh, J. Electrochem. Soc. 144 (1997) 3342.
[2] G. Amatucci, C.N. Schmuts, A. Blyr, C. Sigala, A.S. Gozdz, D. Larcher, J.-M. Tarascon, J. Power Sources 69 (1997) 11.
[3] A.D. Pasquier, A. Blyr, P. Courjal, D. Larcher, G. Amatucci, B. Gerand, J.-M. Tarascon, J. Electrochem. Soc. 146 (1999) 428.
[4] Y. Xia, Y. Zhou, M. Yoshio, J. Electrochem. Soc. 144 (1997) 2593.
[5] S.-T. Myung, S. Komaba, N. Kumagai, J. Electrochem. Soc. 148 (2001) A482.
[6] S. Komaba, N. Kumagai, T. Sasaki, Y. Miki, Electrochemistry 69 (2001) 784.
[7] N. Kumagai, S. Komaba, Y. Kataoka, M. Koyanagi, Chem. Lett. (2000) 1154.
[8] S. Komaba, N. Kumagai, Y. Kataoka, Electrochim. Acta 47 (2002) 1229.
[9] T. Osaka, T. Momma, T. Tajima, Y. Matsumoto, J. Electrochem. Soc. 142 (1995) 1057.
[10] S. Shiraishi, K. Kanamura, Z. Takehara, J. Electrochem. Soc. 146 (1999) 1633.
[11] S. Shiraishi, K. Kanamura, Z. Takehara, J. Appl. Electrochem. 29 (1999) 867–879.
[12] S. Shiraishi, K. Kanamura, Z. Takehara, J. Appl. Electrochem. 25 (1995) 584–591.
[13] M. Ishikawa, S. Yoshitake, M. Morita, Y. Matsuda, J. Electrochem. Soc. 141 (1994) L159.
[14] M. Ishikawa, S. Machino, M. Morita, J. Power Sources 473 (1999) 279.
[15] G.H. Wrodnigg, J.O. Besenhard, M. Winter, J. Electrochem. Soc. 146 (1999) 470.
[16] Sanyo Co., Jpn. Kokai Tokkyo Koho 3066126 (1993).
[17] Ph. Bioensan, J.M. Bodet, F. Perton, M. Broussely, C. Jehoulet, S. Barusseau, S. Herreyre, B. Simon, in: Proceedings of the 10th International Meeting on Lithium Batteries, Abstract No. 286, Como, Italy, 2000.
[18] X. Zhang, R. Kostecki, T.J. Richardson, J.K. Pugh, P.N. Ross Jr., J. Electrochem. Soc. 148 (2001) A1341.
[19] Z.X. Shu, R.S. McMillan, J.J. Murray, I.J. Davidson, J. Electrochem. Soc. 143 (1997) 2230.
[20] K. Shahi, J.B. Wagner, B.B. Owens, in: J.-P. Gabano (Ed.), Lithium Batteries, Academic Press, London, 1983, p. 418.
[21] H. Wang, M. Yoshio, J. Power Sources 101 (2001) 35.